International Journal of Mass Spectrometry 292 (2010) 14–22

Contents lists available at ScienceDirect

International Journal of Mass Spectrometry

journal homepage: www.elsevier.com/locate/ijms

Absolute cross-sections for dissociative photoionization of some small esters

Juan Wang[a], Bin Yang[a], Terrill A. Cool[a,*], Nils Hansen[b]

[a] School of Applied and Engineering Physics, Cornell University, 228 Clark Hall, Ithaca, NY 14853, USA
[b] Combustion Research Facility, Sandia National Laboratories, Livermore, CA 94551, USA

ARTICLE INFO

Article history:
Received 10 December 2009
Received in revised form 10 February 2010
Accepted 11 February 2010
Available online 20 February 2010

Keywords:
Photoionization cross-section
Ester
Biofuel
Photoionization mass spectrometry (PIMS)
Combustion chemistry

ABSTRACT

The first measurements of absolute cross-sections for near-threshold molecular and dissociative photoionization are presented for 11 small esters (methyl formate, ethyl formate, vinyl acetate, methyl propanoate, ethyl propanoate, methyl butanoate, methyl isobutanoate, methyl propenoate, ethyl propenoate, methyl crotonate, and methyl methacrylate). Photoionization mass spectrometry (PIMS) is employed with an energy resolution of 40 meV (fwhm) using a monochromated VUV synchrotron light source. An extensive literature exploring isomerization/dissociation mechanisms is available for six of these molecules. There are, however, no previous observations of dissociative ionization for four simple monounsaturated esters (methyl propenoate, ethyl propenoate, methyl crotonate, and methyl methacrylate), and dissociative ionization of ethyl propanoate has received scant attention. Appearance energies for dissociative photofragment ions of these five molecules are presented.

1. Introduction

Clean-burning renewable oxygenated bio-derived fuels are potentially important additives to, or replacements for, conventional gasoline and diesel fuels, which may reduce dependence on imported petroleum and lower net greenhouse-gas emissions. Biodiesel fuels are an important class of biofuels primarily composed of large methyl and/or ethyl esters derived from vegetable oils and animal fats. These methyl and ethyl esters have the formulas R–(C=O)OCH_3 and R–(C=O)OCH_2CH_3, respectively, where the radical R contains as many as 16–18 carbon atoms in a long chain.

The combustion chemistry of biofuels is poorly understood in comparison with that of conventional hydrocarbons. Kinetic models of the flame chemistry of small alkyl esters provide a first step in the creation of predictive models for the combustion of practical biodiesel fuels [1–8]. In the combustion of both hydrocarbon and oxygenated hydrocarbon fuels, different isomeric forms of the reaction intermediates often follow quite different reaction pathways; therefore experimental determinations of isomeric compositions are of crucial importance in model development. Photoionization mass spectrometry (PIMS) using monochromated synchrotron radiation, applied to the isomerically selective detection of reaction intermediates in low-pressure premixed flat flames [9–11], is uniquely suited for the development and testing of kinetic models of combustion chemistry [12–15]. The absolute cross-sections for molecular and dissociative photoionization presented here are needed for quantitative flame-sampling molecular beam PIMS studies of the flame chemistry of ester fuels used in the development of modular kinetic models of the combustion of practical biodiesel fuels composed of larger, more complex methyl and ethyl esters.

Dissociative ionization of several small esters has been extensively studied by several groups, using a full range of experimental techniques [16–25]. These studies have focused on the measurement of appearance energies for photofragment ions, the structural identities of these fragments and the dynamic mechanisms responsible for their formation. Dissociative ionization channels often arise from complex isomerization processes in competition with direct bond scission of the parent molecular ion [16–25]. Despite considerable interest in these intrinsic features of dissociative photoionization of esters, absolute photoionization cross-sections have been reported for only methyl and ethyl acetate [26]. In this paper absolute photoionization cross-sections for 11 additional small esters are presented.

2. Selected small esters

Photoionization cross-sections are needed for studies of the flame chemistry of 13 simple ester fuels. These are methyl formate, the methyl acetate and ethyl formate $m/z = 74$ isomers, and the 10 molecules with important structural differences displayed in Fig. 1. These molecules have relatively simple structures compared with those of component fatty acid esters of practical biodiesel fuels, which, because of their low volatility, present challenges for

* Corresponding author. Tel.: +1 607 2554191; fax: +1 607 2557658.
E-mail address: tac13@cornell.edu (T.A. Cool).

1387-3806/$ – see front matter © 2010 Elsevier B.V. All rights reserved.
doi:10.1016/j.ijms.2010.02.010

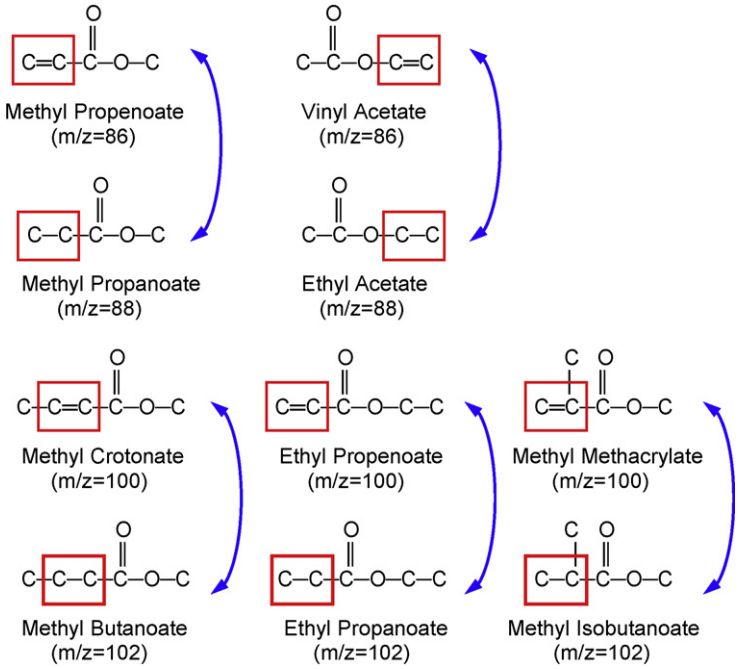

Fig. 1. The influences of unsaturated vs saturated hydrocarbon bonds and effects of chain branching may be studied by comparing the compositions of reaction intermediates for the isomers of $C_4H_6O_2$ ($m/z = 86$) with isomers of $C_4H_8O_2$ ($m/z = 88$), and isomers of $C_5H_8O_2$ ($m/z = 100$) with isomers of $C_5H_{10}O_2$ ($m/z = 102$).

laboratory flame studies. Nevertheless, these molecules are well-suited for study because they contain structural functional groups expected to account for fuel-specific effects in the combustion of more complex biodiesel fuels. These 10 simple esters include 5 saturated molecules paired with 5 monounsaturated analogs of otherwise similar structures highlighted in Fig. 1.

The lowest ionization energies for the saturated esters correspond to removal of an electron from an O-atom lone pair orbital on the carbonyl oxygen. The second ionization energy is from a non-bonding π_2(O–O′) molecular orbital arising from the p-orbitals of the carbonyl and ester O-atoms, localized on the ester oxygen [27,28]. For the five small monounsaturated esters, the first and second ionization energies correspond, respectively to ionization from the π(C=C) orbital and the O-atom lone pair orbital on the carbonyl oxygen [29]. The first and second ionization energies for small esters typically differ by less than 1 eV [28,29]. Esters exhibit complex photoelectron spectra with overlapping contributions from closely spaced bands similar to the spectra of alkanes [27–30]. This gives rise to near-threshold total photoionization cross-sections that increase in quasi-linear fashion [26,31–34].

3. Experimental

3.1. Apparatus

The experimental apparatus and measurement procedures used in these experiments are described in detail elsewhere [26]. A molecular-beam time-of-flight photoionization mass spectrometer is used for the measurements. In brief, the apparatus consists of a low pressure (ca. 15 Torr) stainless steel sample reservoir, a two-stage differentially pumped molecular beam sampling system, and a 1.3 m linear time-of-flight mass spectrometer (TOFMS) with a mass resolution $m/\Delta m = 400$. It is coupled to a 3-m monochromator used to disperse synchrotron radiation at the Advanced Light Source (ALS) of the Lawrence Berkeley National Laboratory [35]. Higher order diffraction and high-energy undulator harmonics are suppressed by passing the undulator beam through a gas filter containing 30 Torr of argon [36]. The monochromator, with a 600 lines/mm iridium-on-copper grating, delivers a dispersed photon beam, tunable over the useful range from 8 to 17 eV with a typical photon current of 5×10^{13} photons/s. The energy resolution of 40 meV (fwhm) matches that used in current PIMS studies of ester flame chemistry [1,37]. Photon energies are calibrated [10] by recording mass spectra at higher (25–30 meV) energy resolution for O_2^+ photo-ions for energies ranging from 12 to 13.2 eV, an interval that contains several narrow autoionization resonances [38]. A probable uncertainty of $\pm$15 meV is assigned to photon energies over the energy ranges of the present measurements.

The sources of the chemicals used in these studies are as follows: methyl formate 99% (Sigma–Aldrich), ethyl formate 97% (Sigma–Aldrich), methyl acetate 99.5% (Sigma–Aldrich), ethyl acetate 99.5+% (Sigma–Aldrich), vinyl acetate 99+% (Aldrich), methyl propanoate 99% (Aldrich), ethyl propanoate 99% (Aldrich), methyl butanoate 99% (Aldrich), methyl isobutanoate 99% (Aldrich), methyl propenoate 99% (Aldrich), ethyl propenoate 99% (Aldrich), methyl crotonate 98% (Aldrich), and methyl methacrylate 99% (Aldrich).

3.2. Measurement procedures

Near-threshold photoionization cross-sections for "target" species of interest are determined by calibration of photo-ion signals from the target species against those of "standard" species with known photoionization cross-sections. Propene is a convenient calibration standard for which absolute total photoionization cross-sections have been accurately measured over the photon energy range from 9.7 to 11.75 eV [39,40]. Binary mixtures of a given ester target molecule with propene are prepared in a 3.8 l stainless steel sample cylinder with a Teflon coated inner surface. Nominal sample mixture compositions consist of ca. 10 Torr each of the ester and propene to which 2300 Torr of argon diluent is added. The samples are allowed to mix for at least 8 h and then are introduced as a cold flow to the sample reservoir at a flow rate of 0.1 slm (standard liters per minute) along with a second flow of argon at 0.15 slm.

The slowly flowing gas mixture in the reservoir at a pressure of 15 Torr is sampled by rapid expansion through the 0.2 mm orifice of a quartz cone to a pressure ca. 10^{-5} Torr. A conical nickel skimmer of 2 mm aperture located on the axis of the expanded flow creates a molecular beam entering a differentially pumped (5×10^{-7} Torr) ionization region between the acceleration plates of the TOFMS, where it is crossed by the dispersed VUV light from the monochromator.

Photo-ions extracted by pulse-gating the repeller plate are propelled along the flight tube of the TOFMS, where they are detected by a microchannel plate (Burle, APD). Ion counts as a function ion flight times (15,008 channels of 2 ns bin width) are recorded for 5×10^5 to 2×10^6 sweeps of a multichannel scaler (Fast ComTek P7886). The resulting mass spectra (ion signal vs m/z), obtained from accumulated ion counts integrated over each mass peak, are corrected for background signals and overlapping contributions from ^{13}C isotopomers and finally normalized by the photon current to yield photoionization efficiency (PIE) spectra for both the target molecule and the propene calibration standard.

Absolute photoionization cross-sections for parent ions of the target species are obtained from the PIE spectra for the parent ion and propene with the relationship [26]:

$$\sigma_T(E) = \frac{\sigma_S(E)\,[S_T(E)P_S/S_S(E)P_T]}{R_T/R_S} \quad (1)$$

Here $\sigma_T(E)$ and $\sigma_S(E)$ are the respective energy-dependent photoionization cross-sections for the target and standard molecules, $S_T(E)$ and $S_S(E)$ are the respective photoionization efficiencies, and P_T and P_S are their partial pressures in the sample mixture. The "mass discrimination factor" $[R_T/R_S]$ for the detection of the target relative to propene is the ratio of the mass-dependent response factors R_T and R_S that account for the respective sampling and detection efficiencies for the target and standard molecules [26]. Mass discrimination factors, cf. Fig. S-1 of the supplementary material, are given in Table 1 for several m/z ratios. The values for $m/z \leq 74$ have a probable error of ±10–12%, while those for higher values are subject to an uncertainty of ±15%. Data for vinyl acetate ($m/z = 86$) were recorded with modified ion optics with a mass discrimination factor of 2.1.

Three binary ester/propene sample mixtures were independently prepared for each of the 13 esters. In addition, samples containing only the ester of interest with no admixed propene were studied to determine the dissociative ionization cross-sections. Cross-sections for dissociative photoionization of a target ester at a photon energy E are directly obtained from the ratio of ion signals for a given fragment ion to that of the parent ion multiplied by the parent ion photoionization cross-section. In the case of methyl propenoate a fragment ion for $m/z = 42$ is observed for photon energies above 10.4 eV in the absence of admixed propene. This required correction of the $m/z = 42$ ion signals for the binary methyl propenoate/propene mixtures above 10.4 eV to account for the fragment ion contribution.

The standard deviations (typically ±10%) for cross-sections determined with the 3 separately prepared sample mixtures yields an estimate of the precision of the present measurements. The cross-sections for the propene calibration standard have uncertainties less than ±15%. An overall uncertainty of ±20% is assigned to the cross-sections reported here.

Table 1
Mass discrimination factors.

m/z	R_T/R_S
60	1.18
74	1.31
86	1.41[a]
88	1.42
100	1.51
102	1.53

[a] For vinyl acetate $R_T/R_S = 2.1$ (see text).

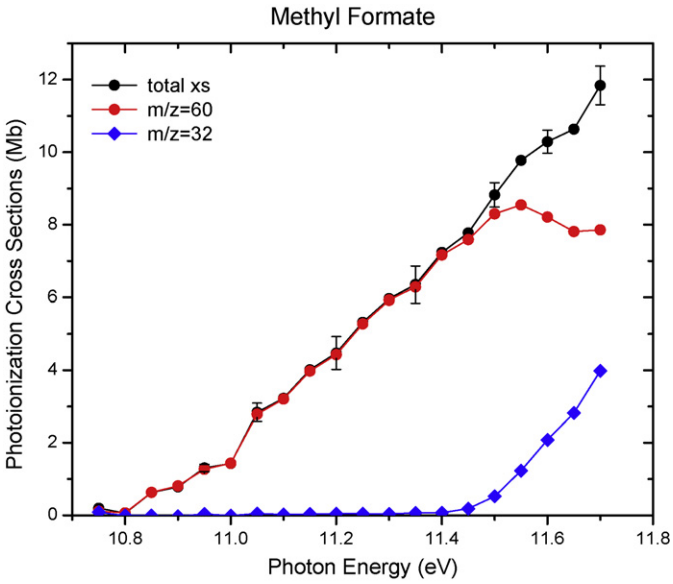

Fig. 2. Molecular and dissociative photoionization cross-sections for methyl formate.

4. Results

4.1. Formates

Dissociative ionization of methyl, ethyl and propyl formates has been extensively studied with a variety of experimental methods [16,18,19,22,24a,24c,25,41]. Zha and coworkers [25] have summarized principal results of earlier work and have presented their studies of the dissociative photoionization of methyl, ethyl and propyl formate with the threshold photoelectron–photo-ion coincidence (TPEPICO) method. Baer and coworkers [24a,c] also report TPEPICO studies of the photoionization of methyl and ethyl formate with reference to earlier work. The structural simplicity of the formate esters facilitates quantitative descriptions of the competition between direct dissociation and dissociation following isomerization of the parent ion, a general feature of dissociative photoionization of esters [24a,c,25].

4.1.1. Methyl formate

The dissociative ionization of methyl formate, the simplest ester, has been extensively investigated [16,19,24c,25a]. The methanol cation, CH_3OH^+, with an appearance energy near 11.45 eV [16,19,25a] formed by dissociation following H-atom migration from formyl to methoxy groups in the parent ion, is the only fragment ion observed for photon energies below 12 eV [25a]. Absolute photoionization cross-sections for the parent and the CH_3OH^+ fragment ions are presented in Fig. 2. The total photoionization cross-section increases in a quasi-linear fashion beyond the onset of fragmentation at ca. 11.45 eV, in the vicinity of the second ionization energy for electron removal from the π_2(O–O′) orbital (vertical IE = 11.55 eV [28]).

4.1.2. Ethyl formate

Zha and coworkers have reported extensive TPEPICO studies of the dissociative photoionization of both methyl and ethyl formate [25a,c]. They observe 7 fragment ions for ethyl formate at

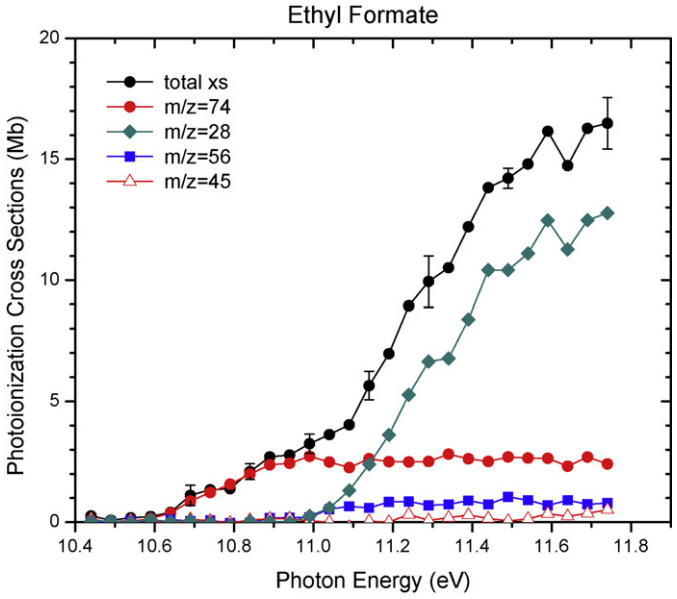

Fig. 3. Molecular and dissociative photoionization cross-sections for ethyl formate.

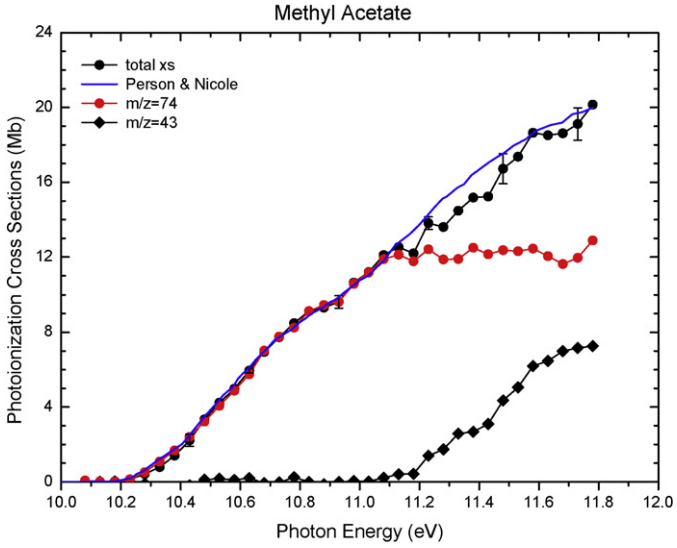

Fig. 4. Molecular and dissociative photoionization cross-sections for methyl acetate [26]. The total photoionization cross-section is compared with the previous measurements of Person and Nicole [39].

m/z = 59, 56, 47, 45, 31, 29 and 28 with appearance energies below 12 eV [25c]. Only the m/z = 28 $C_2H_4^+$, m/z = 56 $C_2H_4CO^+$, and m/z = 45 $C_2H_5O^+$ fragment ions, with cross-sections given in Fig. 3, have signals above background in the present studies. The appearance energies seen for these fragments are in good agreement with the values reported by Zha et al. (10.89 ± 0.05, 10.79 ± 0.05, and 11.40 ± 0.08 eV for m/z = 28, 56, and 45, respectively) [25c]. Godbole and Kebarle [18] and Baer et al. [24a] also observe the

$$HCOOCH_2CH_3^+ \rightarrow CH_2CHC(OH)_2^+ + H \quad (2)$$

dissociation channel with an appearance energy of 11.1 ± 0.1 eV.

The dominant dissociation pathway to $C_2H_4^+$ + HCOOH reflects a competition between rapid direct dissociation of the parent ion and a slow component arising from bond fission from the low-energy distonic intermediate $CH_2CH_2OCHOH^+$ formed by methyl hydrogen transfer to the carbonyl oxygen of the parent ion [16,24a,25c]. The cross-section for $C_2H_4^+$ formation increases monotonically to the 11.75 eV limit of the present studies, while the smaller cross-sections for formation of the m/z = 56 $C_2H_4CO^+$ and m/z = 45 $C_2H_5O^+$ fragments reach nearly constant plateau values ca. 1 Mb and 0.5 Mb, respectively.

4.2. Acetates

4.2.1. Methyl and ethyl acetate

The absolute cross-sections for molecular and dissociative photoionization of methyl and ethyl acetate, previously reported in this journal [26], are displayed here for reference in Figs. 4 and 5. The mechanisms of dissociative ionization of both molecules have been extensively studied [23c,24b,g]. Both exhibit two-component dissociation rates that vary with the internal energy of the parent ion [24b,g]. The only fragment ion of methyl acetate observed for photon energies below 12 eV is the m/z = 43 CH_3CO^+ acetyl cation with an appearance energy of 11.05 eV [42]. The m/z = 59 $C_2H_3O_2^+$ ion reported by Blanchette et al. [23d] with an appearance energy of 11.32 eV was not detected. The identification of the CH_3O/CH_2OH composition of neutral radicals accompanying the acetyl cation has an interesting history [24b,43,44]. Detailed calculations of a $C_3H_6O_2^+$ potential energy surface connecting the parent ion to lower-energy stable intermediate isomer ions, supplemented with RRKM calculations of unimolecular decomposition rates, have been used to model the complex isomerization/dissociation dynamics for comparison with available experiments [24b]. Analysis of TPEPICO measurements reveals that the CH_2OH hydroxymethyl radical is formed at the slow rate, while formation of the CH_3O methoxy radical exhibits both fast and slow rate components. The CH_3O/CH_2OH ratio is predicted to increase with photon energy from its value at threshold of about 3 [24b]; experimental measurements of this ratio as a function of parent ion internal energy are not yet available.

The cross-sections for ethyl acetate of Fig. 5 illustrate that dissociation pathways leading to $C_4H_6O^+$ (m/z = 70) + H_2O and $CH_3C(OH)_2^+$ (m/z = 61) + C_2H_3 predominate below 11.75 eV in agreement with previous studies [23a,24g]. These isomerization/dissociation channels have been extensively studied [18,22,23a,24g]. The ethyl acetate parent ion isomerizes to a lower energy ion of uncertain identity prior to dissociation [23a,24g]. Available evidence suggests that the structure of the $C_4H_6O^+$ (m/z = 70) ion is the methyl vinyl ketone cation $CH_3COCHCH_2^+$

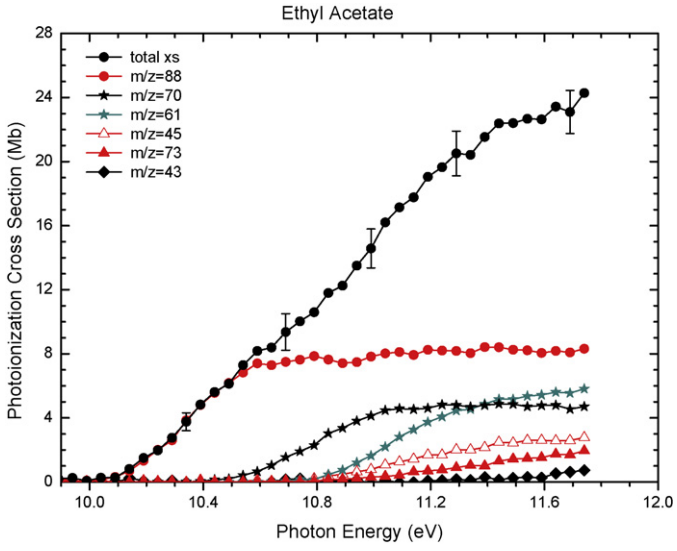

Fig. 5. Molecular and dissociative photoionization cross-sections for ethyl acetate [26].

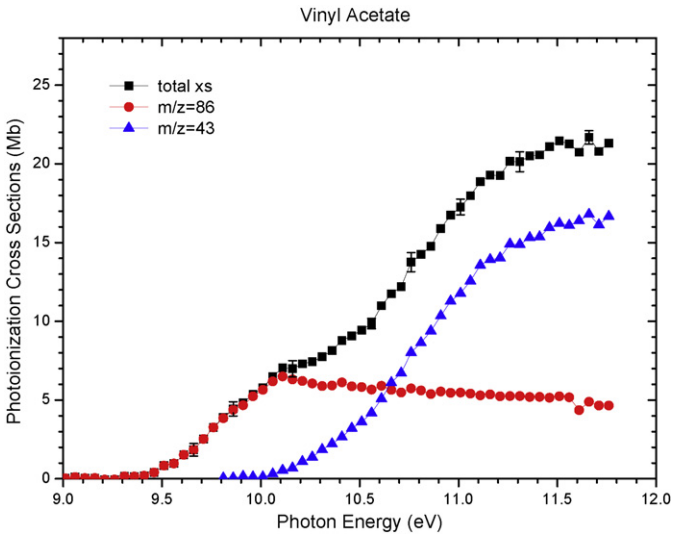

Fig. 6. Molecular and dissociative photoionization cross-sections for vinyl acetate.

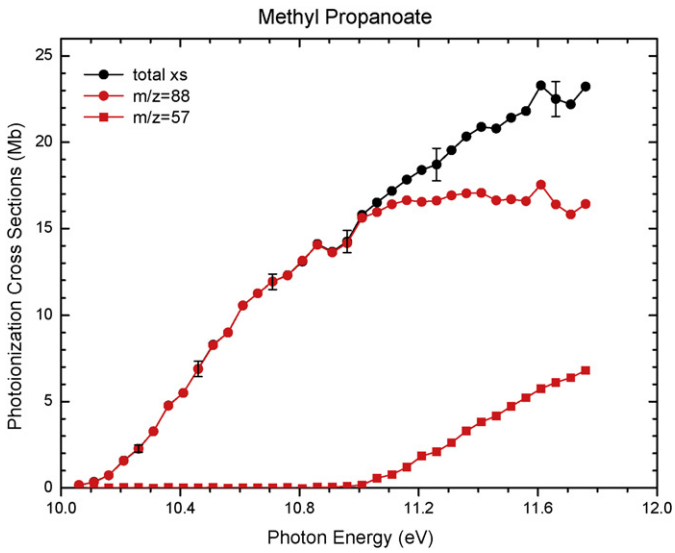

Fig. 7. Molecular and dissociative photoionization cross-sections for methyl propanoate.

[23a,24g,45]. The appearance energies for the fragment ions of Fig. 5 are in good agreement with the accurate measurements of Fraser-Monteiro et al. [24g]. The C_2H_5+ (m/z = 29) ion with an appearance energy of 11.29 eV [24g] was not observable in the present study.

4.2.2. Vinyl acetate

The first ionization energy for vinyl acetate (IE = 9.2 eV) is assigned to ionization from the π(C=C) orbital, while the second and third ionization energies are assigned to lone pair orbitals on the carbonyl (a′) and ester oxygen (a″) atoms, respectively [29]. Methyl acrylate (methyl propenoate) and methyl methacrylate, two other esters with monounsaturated acyl groups, have the same ordering of orbitals [29]. The photoionization cross-section for the vinyl acetate parent ion shown in Fig. 6 rises from an apparent threshold near 9.3 eV to a maximum value ca. 7 Mb at 10.1 eV and then slowly declines on a plateau extending to the 11.75 eV limit of the present measurements. The only ion fragment appearing below 11.75 eV is the CH_3C^+O m/z = 43 acetyl ion identified by Holmes et al. [46] formed in the direct bond fission:

$$[CH_3COOCHCH_2]^+ \rightarrow {}^{\bullet}OCHCH_2 + CH_3C^+O \quad (3)$$

The 9.4 eV ionization threshold seen here exceeds the literature value for the adiabatic ionization energy of 9.2 eV [29,47,48], while the appearance energy for the acetyl ion is in good agreement with the 10.04 eV value measured by Holmes et al. [46].

4.3. Propanoates and butanoates

4.3.1. Methyl propanoate

The well-characterized isomerization/dissociation dynamics of methyl propanoate is the culmination of careful experiments performed with a full array of available techniques, combined with the development and verification of mechanisms using ab initio calculations of the energies and structures of possible stable isomers and the transition states connecting them [24f]. Two-component dissociation rates are observed reflecting the competition between direct bond cleavage:

$$CH_3CH_2COOCH_3^+ \rightarrow CH_3CH_2CO^+ + OCH_3 \quad (4)$$

and formation of the enol isomer:

$$CH_3CH{=}C(OH)OCH_3^+$$

In contrast to methyl acetate, where both hydroxymethyl and methoxy radicals are formed by direct bond scission, only the methoxy radical is produced in the cleavage of methyl propanoate [24f]. The appearance energy of the m/z = 57 $CH_3CH_2CO^+$ ion shown in Fig. 7, measured by Traeger [49] is 10.78 eV. No other fragment ions are observed below the 11.75 eV limit of the present work.

4.3.2. Ethyl propanoate

Surprisingly, in contrast to methyl propanoate, no extensive studies of the dissociative ionization of ethyl propanoate have been reported. The parent ion threshold for ethyl propanoate displayed in Fig. 8 is in good agreement with the value of 10.00 ± 0.02 eV measured by Watanabe et al. [48]. The dissociative photoionization cross-sections for eight fragment ions with appearance energies below 11.75 eV are given in Fig. 8. Approximate (±0.10 eV) appearance energy estimates for these fragments are given in Table 2. The appearance energy for the m/z = 75 $CH_3CH_2C(OH)_2^+$ ion is in good agreement with the 10.77 eV value reported by Godbole and Kebarle [18]; no previous measurements are available for other fragment ions of Table 2, although each of these fragments are

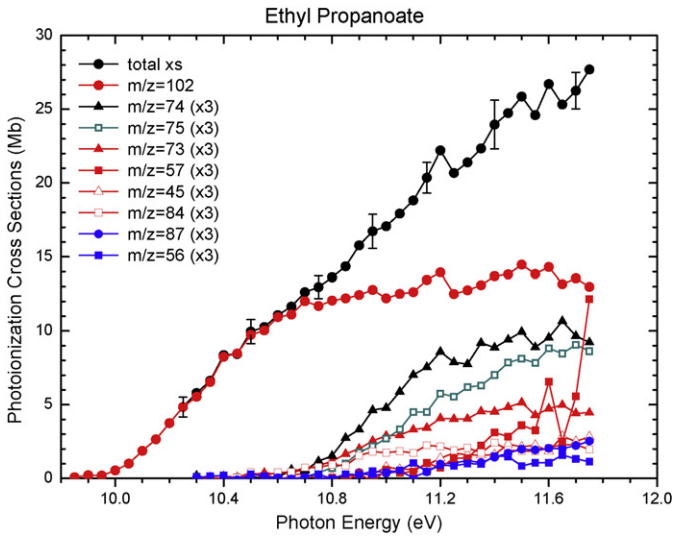

Fig. 8. Molecular and dissociative photoionization cross-sections for ethyl propanoate.

Table 2
Ethyl propanoate.

m/z	Fragments	Appearance energy (eV)
84	$C_5H_8O^+ + H_2O$	10.45 ± 0.1
73	$C_3H_5O_2^+ + C_2H_5$	10.5 ± 0.1
74	$C_3H_6O_2^+ + C_2H_4$	10.6 ± 0.1
75	$CH_3CH_2C(OH)_2^+ + C_2H_3$	10.7 ± 0.1
45	$C_2H_5O^+ + C_2H_5CO$	10.8 ± 0.1
56	$C_3H_4O^+ + C_2H_5OH$	10.85 ± 0.1
87	$C_4H_7O_2^+ + CH_3$	10.9 ± 0.1
57	$C_2H_5CO^+ + C_2H_5O$	11.0 ± 0.1

observed in conventional electron ionization mass spectrometry [50,51]. The dissociative pathways leading to the fragment ions of Table 2 have yet to be determined; thus the suggested neutral species are tentative, subject to revision pending detailed studies of isomerization/dissociation mechanisms.

4.3.3. Methyl butanoate

Dissociative ionization of methyl butanoate has been extensively studied with many experimental methods [21,24e,52]. The $m/z = 74$ $C_3H_6O_2^+$ and $m/z = 71$ $C_4H_7O^+$ fragment ions are prominent with respective appearance energies of 10.18 eV [52] and 11.2 ± 0.2 eV [21]. The structure of the $m/z = 74$ fragment ion was identified by Holmes and Lossing [52] to be the methyl acetate enol ion $CH_2COHOCH_3^+$ formed with the loss of C_2H_4 by direct bond cleavage of the low-energy distonic $CH_2CH_2CH_2COHOCH_3^+$ ion, formed by prior isomerization of the methyl butanoate parent ion. The dissociation dynamics of this mechanism has been quantified by Mazyar and Baer [24e] using ab initio molecular orbital calculations of transition states and RRKM simulations of time-of-flight mass spectra measured with the TPEPICO technique.

Absolute cross-sections for parent ion and dissociative fragment photoionization are presented in Fig. 9. As expected the $m/z = 74$ $C_3H_6O_2^+$ fragment ion appears near 10.2 eV (10.15 ± 0.1 eV), slightly above the adiabatic ionization energy (10.07 ± 0.03 eV [48]; 9.95 ± 0.05 eV [24e]). The $m/z = 74$ fragment ion is the dominant contributor to the total photoionization above 10.4 eV, augmented by the $m/z = 71$ $C_4H_7O^+$ and $m/z = 87$ $C_4H_7O_2^+$ fragment ions with respective appearance energies of 10.9 ± 0.1 and 10.85 ± 0.1 eV. Howe et al. [21] reported an appearance energy of 11.2 ± 0.2 eV for the $m/z = 71$ $C_4H_7O^+$ fragment ion, corresponding to direct loss of the CH_3O radical. The CH_3 radical loss channel associated with

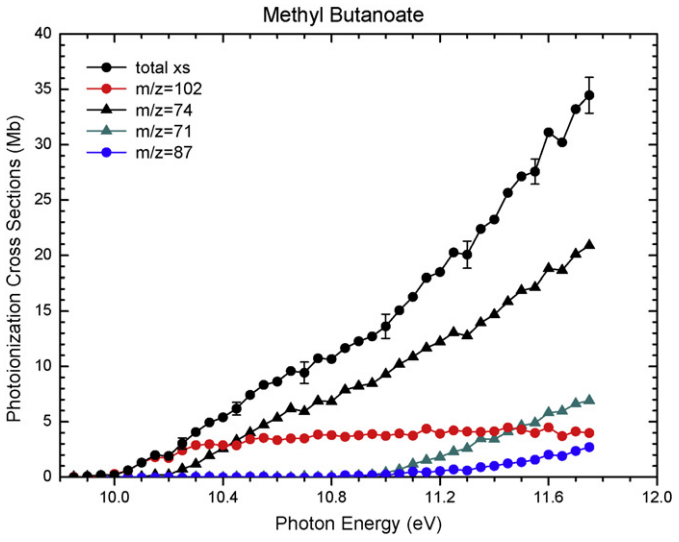

Fig. 9. Molecular and dissociative photoionization cross-sections for methyl butanoate.

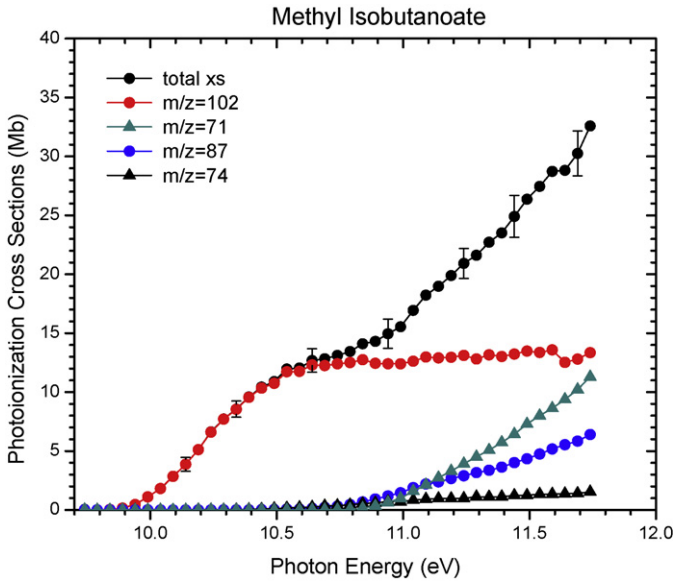

Fig. 10. Molecular and dissociative photoionization cross-sections for methyl isobutanoate.

formation of the $m/z = 87$ $C_4H_7O_2^+$ fragment ion seen here has not been previously reported.

4.3.4. Methyl isobutanoate

Dissociative ionization of methyl isobutanoate has been extensively studied and discussed by Hemberger et al. [53]. The branched structure of the acyl group of methyl isobutanoate dictates a multistep rearrangement sequence leading to the formation of the $m/z = 74$ $CH_2COHOCH_3^+$ methyl acetate enol ion with the loss of C_2H_4, which is more complex than the simple 1,5-hydrogen shift from methyl to carbonyl oxygen isomerization pathway followed in the dissociative ionization of methyl butanoate.

The absolute cross-section data of Fig. 10 show the diminished importance of C_2H_4 loss relative to CH_3O and CH_3 loss channels in comparison with the cross-sections for methyl butanoate of Fig. 9. The observed parent ion threshold ionization energy is in good agreement with the 9.86 eV value reported by Burgers et al. [23b]. The cross-section for formation of the $m/z = 74$ methyl acetate enol ion increases quite slowly from a poorly defined onset with an appearance energy in the 10.2–10.4 eV range. The appearance energies for the $m/z = 71$ and $m/z = 87$ fragment ions of Fig. 10 are 10.75 ± 0.1 and 10.50 ± 0.1 eV, respectively. The latter value exceeds the 10.28 eV appearance energy of Ref. [32b]. The $m/z = 43$ $C_3H_7^+$ propyl ion associated with loss of the $^\bullet C(O)OCH_3$ radical at an appearance energy of 11.42 eV [54], was not observed in our measurements. The cross-sections of Fig. 10 for the loss channels increase in the order $CH_3O > CH_3 > C_2H_4$ above 11.1 eV, in contrast to the $C_2H_4 > CH_3O > CH_3$ ranking for methyl butanoate seen in Fig. 9.

4.4. Esters with monounsaturated acyl groups

4.4.1. Methyl propenoate

The parent ion cross-section data of Fig. 11 for methyl propenoate reveal a threshold of 10.0 ± 0.05 eV in good agreement with an adiabatic ionization energy estimate provided by the photoelectron spectra of Van Dam and Oskam [29]. Dissociative ionization of methyl propenoate has not been previously studied.

The data of Fig. 11 reveal extensive fragmentation above 10.3 eV. Table 3 presents appearance energies and tentative identifications of six dissociative ionization channels.

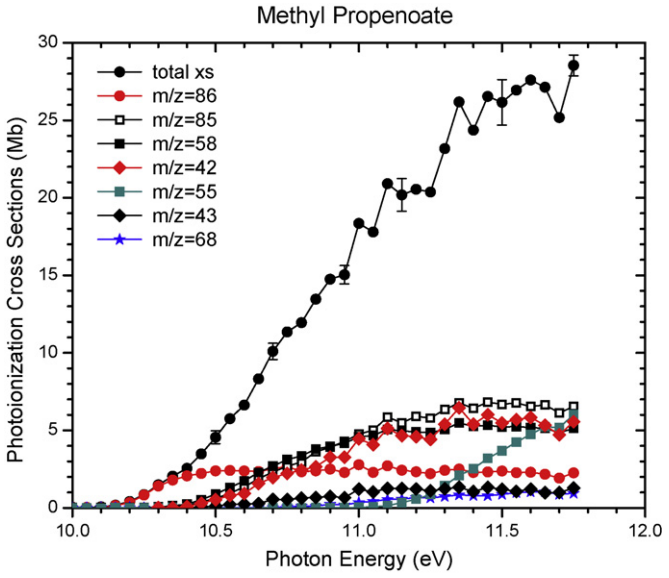

Fig. 11. Molecular and dissociative photoionization cross-sections for methyl propenoate.

Table 3
Methyl propenoate.

m/z	Fragments	Appearance energy (eV)
58	$C_2H_2O_2^+ + C_2H_4$	10.25 ± 0.1
85	$C_4H_5O_2^+ + H$	10.3 ± 0.1
42	$C_2H_2O^+ + C_2H_4O$	10.35 ± 0.1
43	$C_2H_3O^+ + C_2H_3O$	10.4 ± 0.1
68	$C_4H_4O^+ + H_2O$	10.4–10.6
55	$C_3H_3O^+ + CH_3O$	10.95 ± 0.1

Table 4
Ethyl propenoate.

m/z	Fragments	Appearance energy (eV)
56	$C_3H_4O^+ + C_2H_4O$	10.0 ± 0.1
85	$C_4H_5O_2^+ + CH_3$	10.3 ± 0.1
54	$C_3H_2O^+ + C_2H_5OH$	10.3 ± 0.1
43	$C_2H_3O^+ + C_3H_5O$	10.3 ± 0.1
99	$C_5H_7O_2^+ + H$	10.4 ± 0.1
82	$C_5H_6O^+ + H_2O$	10.4 ± 0.1
58	$C_3H_6O^+ + C_2H_2O$	10.4 ± 0.1
72	$C_3H_4O_2^+ + C_2H_4$	10.5 ± 0.1
55	$C_3H_3O^+ + C_2H_5O$	10.5 ± 0.1
73	$C_3H_5O_2^+ + C_2H_3$	10.85 ± 0.1

4.4.2. Ethyl propenoate

The ionization energy of ethyl propenoate is 10.0 ± 0.1 eV as shown in Fig. 12. This is somewhat below the earlier estimate (IE > 10.3 eV) of Morizur et al. [55]. We present here the first observations of the dissociative photoionization of ethyl propenoate. Ten fragment ions are observed for photon energies below 11.75 eV with approximate appearance energies given in Table 4. The identifications of the fragmentation channels given in Table 4 are subject to revision pending detailed studies of isomerization/dissociation mechanisms.

4.4.3. Methyl crotonate

This appears to be the first study of the photoionization of methyl crotonate. Fig. 13 reveals an adiabatic ionization energy of 9.75 ± 0.1 eV for the removal of an electron from the π(C=C) bond. Two direct dissociation channels:

$$C_5H_8O_2^+ \quad (m/z = 100) \rightarrow C_4H_5O_2^+ \quad (m/z = 85) + CH_3$$

$$C_5H_8O_2^+ \quad (m/z = 100) \rightarrow C_4H_5O^+ \quad (m/z = 69) + CH_3O$$

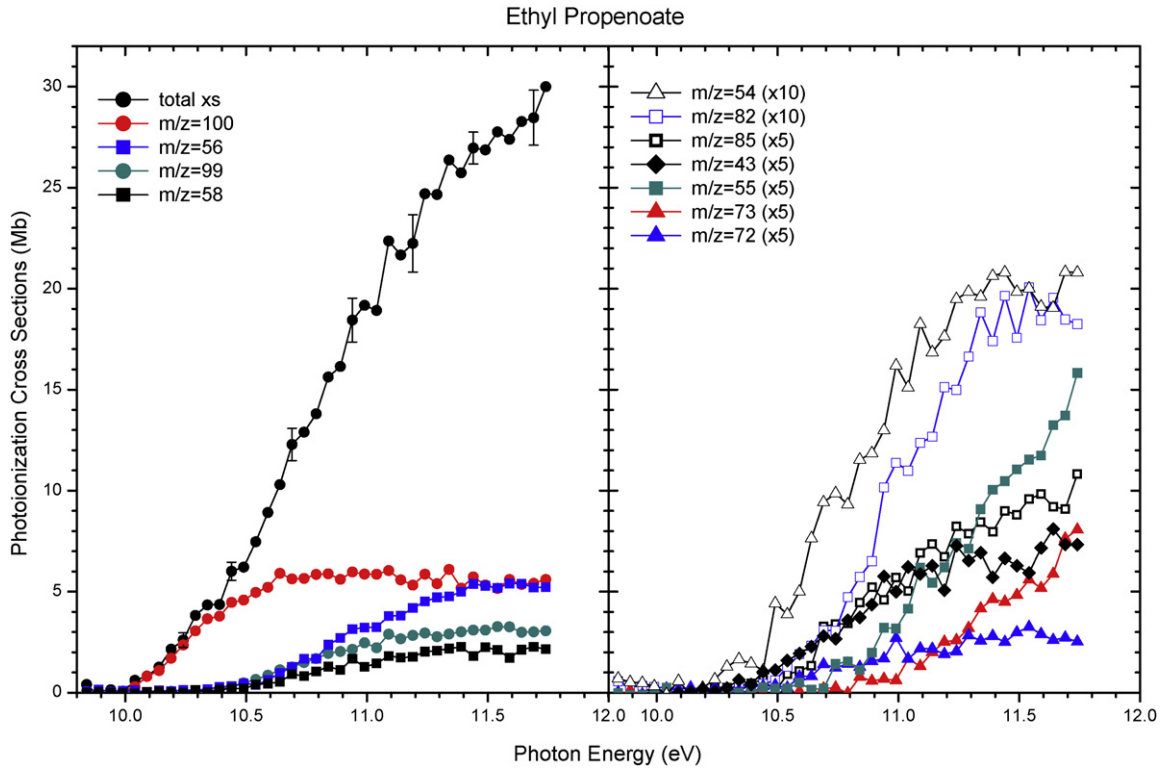

Fig. 12. Molecular and dissociative photoionization cross-sections for ethyl propenoate.

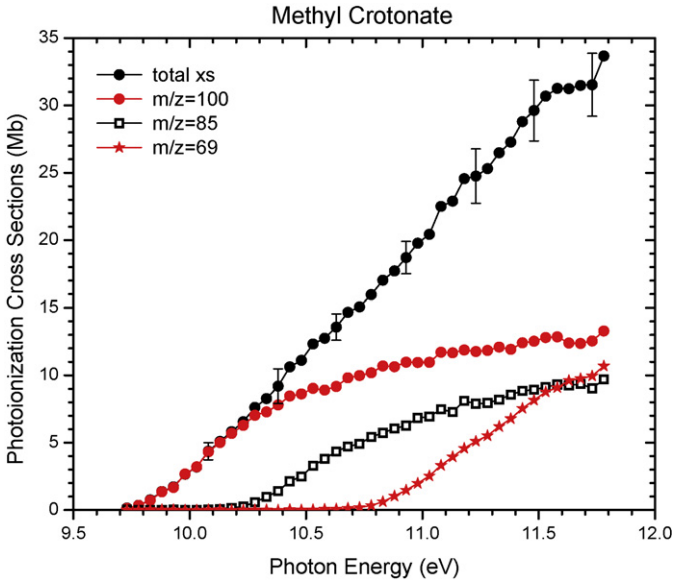

Fig. 13. Molecular and dissociative photoionization cross-sections for methyl crotonate.

yielding the CH_3 and CH_3O neutral fragments are seen with respective ionization energies of 10.1 ± 0.1 and 10.6 ± 0.1 eV.

4.4.4. Methyl methacrylate

The dissociative ionization of methyl methacrylate has not been previously studied. Fig. 14 displays parent ion cross-sections exhibiting an adiabatic ionization energy of 9.7 ± 0.1 eV in agreement with the photoelectron spectra of Van Dam and Oskam [29]. A plateau in the parent ion cross-section is reached near 10.7 eV, which stretches to the 11.75 eV limit of the present measurements. Extensive fragmentation is observed above 10.3 eV. The appearance energies for the observed dissociative ionization channels are given in Table 5. The prominent dissociation channels leading to CH_3 and CH_3O radicals seen for methyl crotonate are also present for methyl methacrylate.

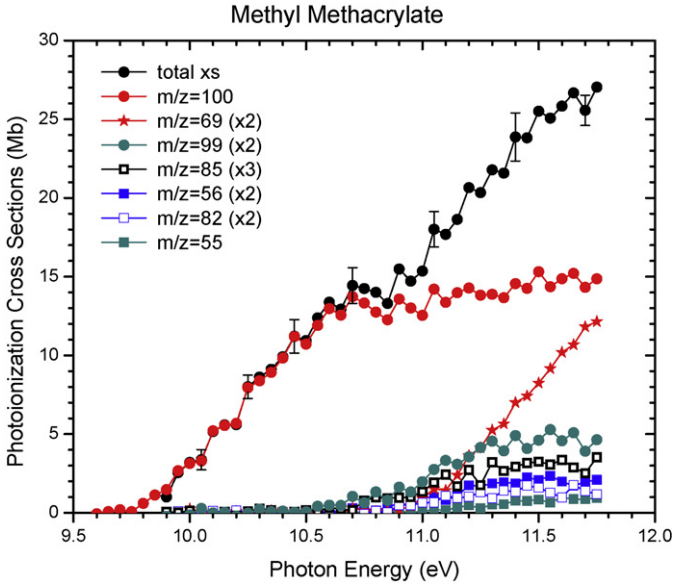

Fig. 14. Molecular and dissociative photoionization cross-sections for methyl methacrylate.

Table 5
Methyl methacrylate.

m/z	Fragments	Appearance energy (eV)
85	$C_4H_5O_2^+ + CH_3$	10.3 ± 0.1
56	$C_3H_4O^+ + C_2H_4O$	10.3 ± 0.1
99	$C_5H_7O_2^+ + H$	10.4 ± 0.1
69	$C_4H_5O^+ + CH_3O$	10.75 ± 0.1
55	$C_3H_3O^+ + C_2H_5O$	10.8 ± 0.1
82	$C_5H_6O^+ + H_2O$	10.85 ± 0.1

5. Conclusion

This paper presents the first measurements of near-threshold cross-sections for molecular and dissociative photoionization for 11 simple esters. The total photoionization cross-sections and cross-sections for parent and fragment ion formation for these eleven esters, and for methyl acetate and ethyl formate reported previously [26], exhibit qualitative features similar to those found for simple alkanes. The photoelectron spectra of these esters are complex with overlapping contributions from closely spaced bands. Their total photoionization cross-sections rise gradually from threshold in a quasi-linear fashion, with major contributions from numerous dissociative ionization channels. The parent ion cross-sections rise to plateaus at photon energies coincident with the onset of dissociative photoionization (typically $\lesssim$ 0.5–0.8 eV above threshold), which extend to the 11.75 eV limit of the present studies.

An extensive literature exploring isomerization/dissociation mechanisms is available for eight of these molecules (methyl formate, ethyl formate, methyl acetate, ethyl acetate, vinyl acetate, methyl propanoate, methyl butanoate, and methyl isobutanoate).

However, dissociative ionization of ethyl propanoate has received scant attention and no previous observations of dissociative ionization are available for four simple monounsaturated esters: methyl propenoate, ethyl propenoate, methyl crotonate, and methyl methacrylate. Appearance energies and tentative identifications of dissociative photoionization products are presented here for these five molecules, although definitive studies of dissociation mechanisms with a variety of experimental techniques are clearly needed. Indeed, the appearance of numerous pathways for dissociative photoionization at photon energies just above the adiabatic ionization energies for these molecules makes them interesting candidates for detailed studies of isomerization/dissociation mechanisms.

The photoionization cross-sections reported here are presented in tabular form in the supplementary material.

Acknowledgements

The authors thank Tina Kasper for helpful discussions and are grateful to Paul Fugazzi for expert technical assistance. This work is supported by the Division of Chemical Sciences, Geosciences, and Biosciences, the Office of Basic Energy Sciences, the U.S. Department of Energy, in part under grant DE-FG02-01ER15180. Sandia is a multi-program laboratory operated by Sandia Corporation, a Lockheed Martin Company, for the National Nuclear Security Administration under contract DE-AC04-94-AL85000. The Advanced Light Source is supported by the Director, Office of Science, Office of Basic Energy Sciences, Materials Sciences Division, of the U.S. Department of Energy under Contract No. DE-AC02-05CH11231 at Lawrence Berkeley National Laboratory.

Appendix A. Supplementary data

Supplementary data associated with this article can be found, in the online version, at doi:10.1016/j.ijms.2010.02.010.

References

[1] C.K. Westbrook, W.J. Pitz, P.R. Westmoreland, F.L. Dryer, M. Chaos, P. Oßwald, K. Kohse-Höinghaus, T.A. Cool, J. Wang, B. Yang, N. Hansen, T. Kasper, Proc. Combust. Inst. 32 (2009) 221.
[2] S. Gaïl, S.M. Sarathy, S.A. Syed, P. Dagaut, P. Diévart, A.J. Marchese, F.L. Dryer, Proc. Combust. Inst. 31 (2007) 305.
[3] P. Dagaut, S. Gaïl, M. Sahasrabudhe, Proc. Combust. Inst. 31 (2007) 2955.
[4] S. Dooley, H.J. Curran, J.M. Simmie, Combust. Flame 153 (2008) 2.
[5] O. Herbinet, W.J. Pitz, C.K. Westbrook, Combust. Flame 154 (2008) 507.
[6] S. Gaïl, S.M. Sarathy, M.J. Thomson, P. Diévart, P. Dagaut, Combust. Flame 155 (2008) 635.
[7] C.J. Hayes, D.R. Burgess Jr., Proc. Combust. Inst. 32 (2009) 263.
[8] K. Seshadri, T. Lu, O. Herbinet, S. Humer, U. Niemann, W.J. Pitz, R. Seiser, C.K. Law, Proc. Combust. Inst. 32 (2009) 1067.
[9] T.A. Cool, K. Nakajima, T.A. Mostefaoui, F. Qi, A. McIlroy, P.R. Westmoreland, M.E. Law, L. Poisson, D.S. Peterka, M. Ahmed, J. Chem. Phys. 119 (2003) 8356.
[10] T.A. Cool, A. McIlroy, F. Qi, P.R. Westmoreland, L. Poisson, D.S. Peterka, M. Ahmed, Rev. Sci. Instrum. 76 (2005) 094102.
[11] F. Qi, R. Yang, B. Yang, C. Huang, L. Wei, J. Wang, L. Sheng, Y. Zhang, Rev. Sci. Instrum. 77 (2006) 084101.
[12] N. Hansen, T.A. Cool, P.R. Westmoreland, K. Kohse-Höinghaus, Prog. Energy Combust. Sci. 35 (2009) 168.
[13] N. Hansen, S.J. Klippenstein, C.A. Taatjes, J.A. Miller, J. Wang, T.A. Cool, B. Yang, R. Yang, L. Wei, C. Huang, J. Wang, F. Qi, M.E. Law, P.R. Westmoreland, J. Phys. Chem. A 110 (2006) 3670.
[14] N. Hansen, S.J. Klippenstein, J.A. Miller, J. Wang, T.A. Cool, M.E. Law, P.R. Westmoreland, T. Kasper, K. Kohse-Höinghaus, J. Phys. Chem. A 110 (2006) 4376.
[15] N. Hansen, J.A. Miller, P.R. Westmoreland, T. Kasper, K. Kohse-Höinghaus, J. Wang, T.A. Cool, Combust. Flame 156 (2009) 2153.
[16] A.B. King, F.A. Long, J. Chem. Phys. 29 (1958) 374.
[17] F.W. McLafferty, Anal. Chem. 31 (1959) 82.
[18] E.W. Godbole, P. Kebarle, Trans. Faraday Soc. 58 (1962) 1897.
[19] D. Van Raalte, A.G. Harrison, Can. J. Chem. 41 (1963) 2054.
[20] M.S.B. Munson, F.H. Field, J. Am. Chem. Soc. 88 (1966) 4337.
[21] I. Howe, D.H. Williams, D.G.I. Kingston, H.P. Tannenbaum, J. Chem. Soc. (B) (1969) 439.
[22] F.M. Benoit, A.G. Harrison, F.P. Lossing, Org. Mass Spectrom. 12 (1977) 78.
[23] (a) J.L. Holmes, P.C. Burgers, J.K. Terlouw, Can. J. Chem. 59 (1981) 1805;
(b) P.C. Burgers, J.L. Holmes, F.P. Lossing, F.R. Povel, J.K. Terlouw, Org. Mass Spectrom. 18 (1983) 335;
(c) J.L. Holmes, F.P. Lossing, Org. Mass Spectrom. 14 (1979) 512;
(d) M.C. Blanchette, J.L. Holmes, C.E.C.A. Hop, F.P. Lossing, R. Postma, J.A. Ruttink, J.K. Terlouw, J. Am. Chem. Soc. 108 (1986) 7589.
[24] (a) T. Baer, O.A. Mazyar, J.W. Keister, P.M. Mayer, Ber. Bunsenges. Phys. Chem. Chem. Phys. 101 (1997) 478;
(b) O.A. Mazyar, P.M. Mayer, T. Baer, Int. J. Mass Spectrom. Ion Proc. 167/168 (1997) 389;
(c) O.A. Mazyar, T. Baer, J. Phys. Chem. A 102 (1998) 1682;
(d) O.A. Mazyar, T. Baer, J. Am. Soc. Mass Spectrom. 10 (1999) 200;
(e) O.A. Mazyar, T. Baer, Int. J. Mass Spectrom. 185/186/187 (1999) 165;
(f) O.A. Mazyar, T. Baer, J. Phys. Chem. A 103 (1999) 1221;
(g) L. Fraser-Monteiro, M.L. Fraser-Monteiro, J.L. Butler, T. Baer, J. Phys. Chem. 86 (1982) 752.
[25] (a) T. Nishimura, Q. Zha, G.G. Meisels, J. Chem. Phys. 87 (1987) 4589;
(b) Q. Zha, R.N. Hayes, T. Nishimura, G.G. Meisels, M.L. Gross, J. Phys. Chem. 94 (1990) 1286;
(c) Q. Zha, T. Nishimura, G.G. Meisels, Int. J. Mass Spectrom. Ion Proc. 120 (1992) 85.
[26] J. Wang, B. Yang, T.A. Cool, N. Hansen, T. Kasper, Int. J. Mass Spectrom. 269 (2008) 210.
[27] U. Mölder, I.K. Koppel, P. Burk, R. Pikver, Int. J. Quantum Chem. 62 (1997) 303.
[28] D.A. Sweigart, D.W. Turner, J. Am. Chem. Soc. 94 (1972) 5592.
[29] H. Van Dam, A. Oskam, J. Electron. Spectrosc. Relate. Phenom. 13 (1978) 273.
[30] K. Kimura, S. Katsuma, A.Y.T. Iwata, Handbook of HeI Photoelectron Spectra of Fundamental Organic Compounds, Japan Scientific Soc. Press, Tokyo, 1981.
[31] H. Koizumi, J. Chem. Phys. 95 (1991) 5846.
[32] R.I. Schoen, J. Chem. Phys. 37 (1962) 2032.
[33] W.A. Chupka, J. Berkowitz, J. Chem. Phys. 47 (1967) 2921.
[34] K. Kameta, N. Kouchi, M. Ukai, Y. Hatano, J. Electron. Spectrosc. Relate. Phenom. 123 (2002) 225.
[35] P.A. Heimann, M. Koike, C.W. Hsu, D. Blank, X.M. Yang, A.G. Suits, Y.T. Lee, M. Evans, C.Y. Ng, C. Flaim, H.A. Padmore, Rev. Sci. Instrum. 68 (1997) 1945.
[36] A.G. Suits, P.A. Heimann, X.M. Yang, M. Evans, C.W. Hsu, K.T. Lu, Y.T. Lee, A.H. Kung, Rev. Sci. Instrum. 66 (1995) 4841.
[37] P. Oßwald, U. Struckmeier, T. Kasper, K. Kohse-Höinghaus, J. Wang, T.A. Cool, N. Hansen, P.R. Westmoreland, J. Phys. Chem. A 111 (2007) 4093.
[38] A.J.C. Nicholson, J. Chem. Phys. 39 (1963) 954.
[39] J.C. Person, P.P. Nicole, Argonne National Laboratory Radiological Physics Division Annual Report, July 1969–June 1970, p. 97.
[40] J.C. Person, P.P. Nicole, J. Chem. Phys. 53 (1970) 1767.
[41] D.T. Leeck, K.M. Stirk, L.C. Zeller, L.K.M. Kiminkinen, L.M. Castro, P. Vainiotalo, H.I. Kenttämaa, J. Chem. Soc. 116 (1994) 3028.
[42] J.C. Traeger, R.G. McLoughlin, A.J.C. Nicholson, J. Am. Chem. Soc. 104 (1982) 5318.
[43] N. Heinrich, J. Schmidt, H. Schwarz, Y. Apeloig, J. Am. Chem. Soc. 109 (1987) 1317.
[44] J.L. Holmes, J.K. Terlouw, Org. Mass Spectrom. 21 (1986) 776.
[45] A.N.H. Yeo, Chem. Commun. (1970) 1154.
[46] J.L. Holmes, F.P. Lossing, J.K. Terlouw, J. Am. Chem. Soc. 108 (1986) 1086.
[47] P.J. Linstrom, W.G. Mallard, NIST Chemistry WebBook, NIST Standard Reference Database Number 69, National Institute of Standards and Technology, Gaithersburg, MD, 2003.
[48] K. Watanabe, T. Nakayama, J. Mottl, J. Quant. Spectrosc. Radiat. Transfer 2 (1962) 369.
[49] J.C. Traeger, Org. Mass Spectrom. 20 (1985) 223.
[50] J.H. Beynon, R.A. Saunders, A.E. Williams, Anal. Chem. 33 (1961) 221.
[51] A.G. Sharkey, J.L. Shultz, R.A. Friedel, Anal. Chem. 31 (1959) 87.
[52] J.L. Holmes, F.P. Lossing, J. Am. Chem. Soc. 102 (1980) 1591.
[53] P.H. Hemberger, J.C. Kleingeld, K. Levsen, N. Mainzer, A. Mandelbaum, N.N.M. Nibbering, H. Schwartz, R. Weber, A. Weisz, C. Wesdemitis, J. Am. Chem. Soc. 102 (1980) 3736.
[54] J.C. Holmes, F.P. Lossing, P.M. Mayer, J. Am. Chem. Soc. 113 (1991) 9723.
[55] J.P. Morizur, J. Mercier, M. Sarraf, Org. Mass Spectrom. 17 (1982) 327.